SUBSIDENCE PATTERNS IN THE NIGERIAN SECTOR OF BENIN (DAHOMEY) BASIN: EVIDENCE FROM THREE OFFSHORE WELLS.

Olabode, S. O.
Department of Applied Geology, The Federal University of Technology, Akure. Ondo State, Nigeria.
(Corresponding Author: soolabode@futa.edu.ng; bodesolomon@yahoo.com)
(Received: 20th May, 2015; Accepted: 29th June, 2015)

ABSTRACT

The application of one-dimensional (1-D) backstripping analysis was used to determine subsidence patterns in three offshore wells (Ayetoro – 1, Baba – 1 and Epiya – 1) located in the Nigeria sector of Benin (Dahomey) Basin. Biostratigraphic data obtained in the three wells indicated that the oldest sediment penetrated varied from Cenomanian to Campanian in age while the youngest sediments are Eocene to Neogene in age. Results of subsidence analysis of the Cretaceous to Tertiary sediments revealed four main phases of subsidence, these are (i) Early late Cretaceous phase characterised by accelerated tectonic subsidence and gradual uplift patterns; (ii) Late Cretaceous phase characterised by relatively high uniform rates of subsidence and minor uplift; (iii) Paleogene to Neogene phase was characterised by variable rates of tectonic subsidence and uplift; and (iv) Quaternary phase began with accelerated tectonic subsidence and followed by reduced rates of tectonic subsidence. The results obtained showed that quantitative analysis of tectonic subsidence is feasible in the area of study area.

Keywords: Backstripping, Subsidence and Uplift, Benin (Dahomey) Basin, Cretaceous, Tertiary.

INTRODUCTION

Vertical movements in sedimentary basins during their development in geological time are being constrained by their tectonic subsidence and uplift histories. The techniques of geohistory analysis and backstripping by Van Hinte (1978) and Sclater and Christie (1980) respectively, have proved to be powerful tools in quantifying patterns of tectonic subsidence and uplift. Geohistory analysis has been used to study the vertical response of sedimentary basins to tectonics both in extensional (Sclater and Christie, 1980) and compressional (Coudert *et al*., 1995) tectonic settings. The applications of backstripping technique in passive margin settings have been remarkably successful, especially, in the response of sedimentary basins to the effect of subsidence and uplift.

The application of the backstripping technique to the Nigeria sector of Benin (Dahomey) Basin was performed by Onuoha and Ofuegbu (1987) to infer the Cretaceous – Tertiary subsidence and burial histories. However, the study was constrained by limited number of well (Afowo – 1) located in the shallow offshore area. Recently, new quantitative and qualitative insights have been gained through the application of geohistory and backstripping techniques both on regional and local scale. Such insights include; anomalous subsidence (Ceramicola *et al*., 2005), tectonic control on the architecture of sedimentary facies (Carminati *et al*., 2007) and reconstruction of synsedimentary fault activity (Wagreich and Schmid, 2002).

This paper employed the methods that have been previously used for the recovery of tectonic component of subsidence from fully lithified and siliciclastic sedimentary successions made up of different lithologies. It presents an attempt to quantitatively derive the tectonic subsidence and uplift history in offshore section of Benin Basin where data are available on exploratory wells. The tectonic subsidence and uplift analyses carried out on the three wells cover the entire depositional history of the sediments, which span through Cenomanian and Pleistocene. The three wells were drilled to the top of basement rocks as observed from the ditch cuttings descriptions, but the oldest sediment encountered was Cenomanian.

Geological Setting and Stratigraphy

The Benin (Dahomey) Basin forms one of a series of West African Atlantic Margin basins that were initiated during the period of rifting in the

late Jurassic to early Cretaceous. (Omatsola and Adegoke, 1981; Weber and Daukorou, 1975; Whiteman, 1982). The basin stretches along the coast of Nigeria, Benin Republic, Togo and Ghana in the margin of the Gulf of Guinea (Fig. 1). It is separated from Niger Delta in the Eastern section by Benin Hinge Line and Okitipupa Ridge and marks the continental extension of the chain fracture zone (Wilson and Williams; 1979; Coker and Ejedawe, 1987, Onuoha, 1999). It is bounded on the west by Ghana Ridge, and has been interpreted as the Romanche fracture zone (Whiteman, 1982; Burke *et al.*, 2003). The basin fill covers a broad arc–shaped profile, attaining about 13 km maximum width in the onshore at the basin axis along Nigerian and Republic of Benin boundary. This narrows westwards and eastwards to about 5 km (Coker and Ejedawe, 1987; Coker, 2002).

Detailed geology, evolution, stratigraphy and hydrocarbon occurrence of the basin have been described by Jones and Hockey (1964), Reyment (1965), Adegoke (1969), Omatsola and Adegoke (1981), Coker and Ejedawe (1987), Billman (1992) and Hack *et al.* (2000). Most of these authors have recognized two structural elements, which comprise the Benin basin proper and the Okitipupa structure. Coker and Ejedawe (1987) identified three structural domains; namely, the onshore (Bodashe, Ileppa – Ojo), the Okitipupa structure (Union – Gbekebo) and offshore. They emphasized that these three structural domains have gone through three main stages of basin evolution. These stages are initial graben (pre-drift) phase, prolonged transitional stage and open marine (drift) phase.

Early study on the basin stratigraphy by Jones and Hockey (1964) recognized both Cretaceous and Tertiary sediments (Fig. 2). Other subsequent workers recognized three chronostratigraphic units: (i) pre-lower Cretaceous folded sequence, (ii) Cretaceous sequence and (iii) Tertiary sequence (Omatsola and Adegoke, 1981; Billman, 1992) (Fig. 2). The Cretaceous stratigraphy as compiled from outcrop and borehole records consists Abeokuta Group sub-divided into three informal formational units namely Ise, Afowo

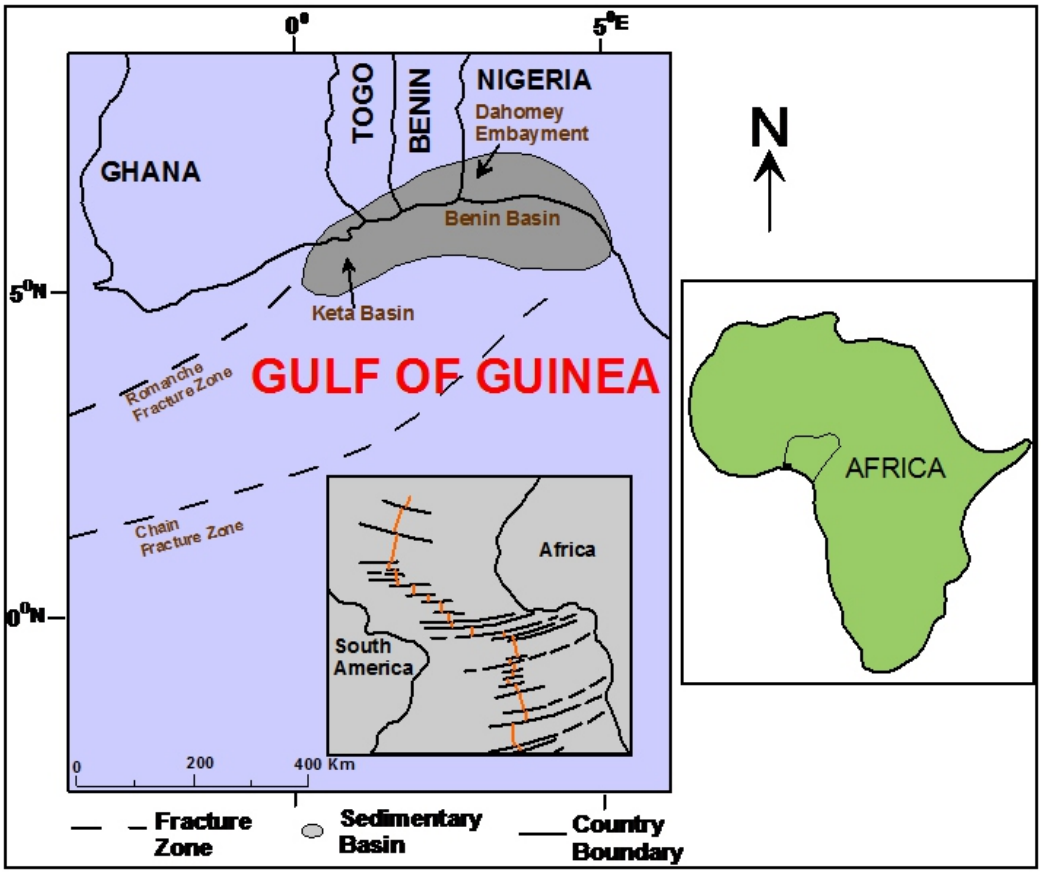

Fig. 1. Regional map of four countries showing the location of the Benin (Dahomey) Basin in the Gulf of Guinea (modified from Brownfield and Chapentier, 2006).

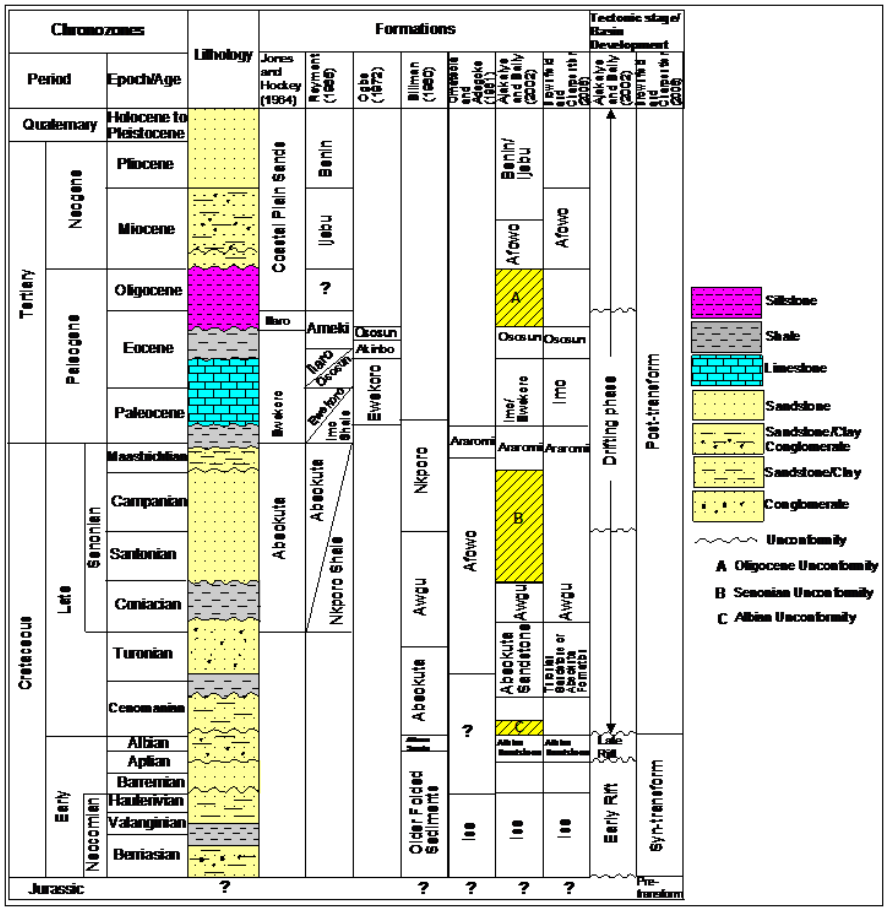

Fig. 2. Stratigraphy of the Nigerian sector of the Benin (Dahomey) Basin.

(Omatsola and Adegoke, 1981). Ise Formation unconformably overlies the basement complex and comprises coarse conglomeratic sediments. Afowo Formation is composed of transitional to marine sands and sandstone with variable but thick interbedded shales and siltstone. Araromi is the uppermost formation and is made up of shales and siltstone with interbeds of limestone and sands (Fig. 2). The Tertiary sediments consist of Ewekoro, Akinbo, Oshosun, Ilaro and Benin (Coastal Plain Sands) Formations (Fig. 2). The Ewekoro Formation is made up of fossiliferous well-bedded limestone while Akinbo and Oshosun Formations are made up of flaggy grey and black shales. Glauconitic rock bands and phosphatic beds define the boundary between Ewekoro and Akinbo Formations. Ilaro and Benin Formations are predominantly coarse sandy estuarine, deltaic and continental beds.

The stratigraphy of the Cretaceous and Tertiary Formations in the Nigerian sector of the basin is controversial. This is due primarily to different stratigraphic names that have been proposed for the same Formation in different localities in the basin (Billman, 1992, Coker, 2002). This situation can be partly blamed on the lack of good borehole coverage and adequate outcrops for detailed stratigraphic studies.

METHODS

The procedure used to calculate the tectonic subsidence in the Nigeria part of Benin Basin located in the Gulf of Guinea which corresponds to a miogeoclinal sedimentation was a modification of backstripping method of Steckler and Watts (1978), Sclater and Christie (1980) and Bond and Kominz (1984). The procedure involved the following stages: (i) successive restoration of stratigraphic sections to their initial thicknesses and bulk densities; (ii) decompaction of stratigraphic sections; and (iii) tectonic subsidence calculation. In the present study, the backstripping technique was applied to three wells located in the offshore section of Benin (Dahomey) Basin (Fig. 3).

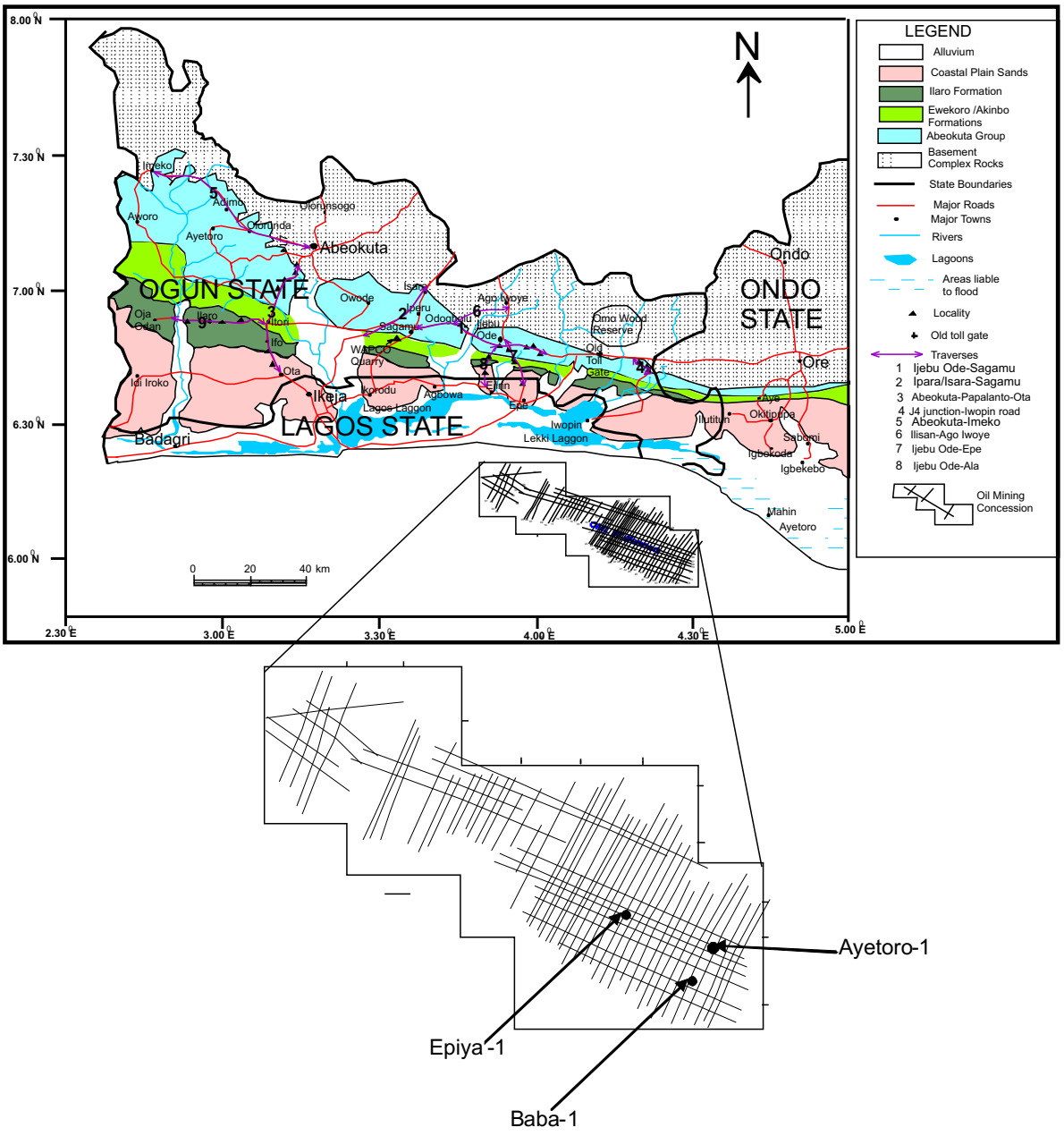

Fig. 3. Geological map of southwestern Nigeria showing the location of three wells in the offshore part used for the backstripping analysis.

The procedure began with restoring the lowest unit in a stratigraphic section to its initial thickness and bulk density, and placing its top at a depth below sea level corresponding to the average water depth in which the unit was deposited. This was followed by removing the isostatic subsidence of the basement caused by the weight of the sediment in the unit. The depth to the surface on which the unit was deposited was recalculated with only the weight of the water as the basement loading factor. This procedure was repeated for all the sedimentary units in the section placing each successively younger unit on top of the previous unit. The variation in paleowater depth and relative sea level changes was included in these calculations.

The backstripping equation was derived by considering a case shown in Figure 4 of two columns of the crust and upper mantle that before and after backstripping are in isostatic equilibrium. If the pressure at the base of the two columns is balanced the equation below will hold:

$$\rho_m g W_{di} + \rho_{si} g S^*_i + \rho_c g = {}_i \rho_w g + \rho_c + x \rho_m g \text{ --- } 1$$

where W_{di}, S^*_I , γ_i are the water depth, de-compacted sediment thickness and tectonic subsidence of the i^{th} stratigraphic layer, respectively, while g is the average gravity and T, ρ_c,ρ_w and ρ_{si} are the mean crustal thickness, crustal density, water density and de-compacted sediment density, respectively. Crustal density and mean crustal thickness are assumed to be constant during the unloading process.

The equation below can also be used to explain Figure 4.

$$X = W_{di} + S^*_i + T(\gamma_i + \Delta_{sli} + T) \quad \text{----------} 2$$

Where Δ_{sli} is the change in relative seal level.

$$\therefore \gamma_i = W_{di} + S^*_i (\rho_m - \rho_{si}) / (\rho_m - \rho_w)\} - \Delta_{sli} \rho_m (\rho_m - \rho_w) \text{----------} 3$$

Equation (3) is the backstripping equation, which allow γ_i to be determined directly from observed stratigraphic data.

The following terms are defined from the equation

W_{di} = water depth

$S^*_I \{ (\rho_m - \rho_{si}) / (\rho_m - \rho_w) \}$ = sediment loading

$\Delta_{sli} \{\rho_m / (\rho_m - \rho_w)$ = sea level loading

For accurate application of the equation it is necessary to determine: (i) the thickness and (ii) density of the sediments in the past before the effect of diagenetic (post-depositional) processes. This is because the observed present thickness of the stratigraphic layer has been affected by post-depositional processes. Since backstripping attempts to correct the stratigraphic record for the effects of loading in the past, it is not sufficient to use the sediment thickness and density of a stratigraphic unit as measured today. The process used to determine the unlithified stratigraphic thickness and density is called de-compaction.

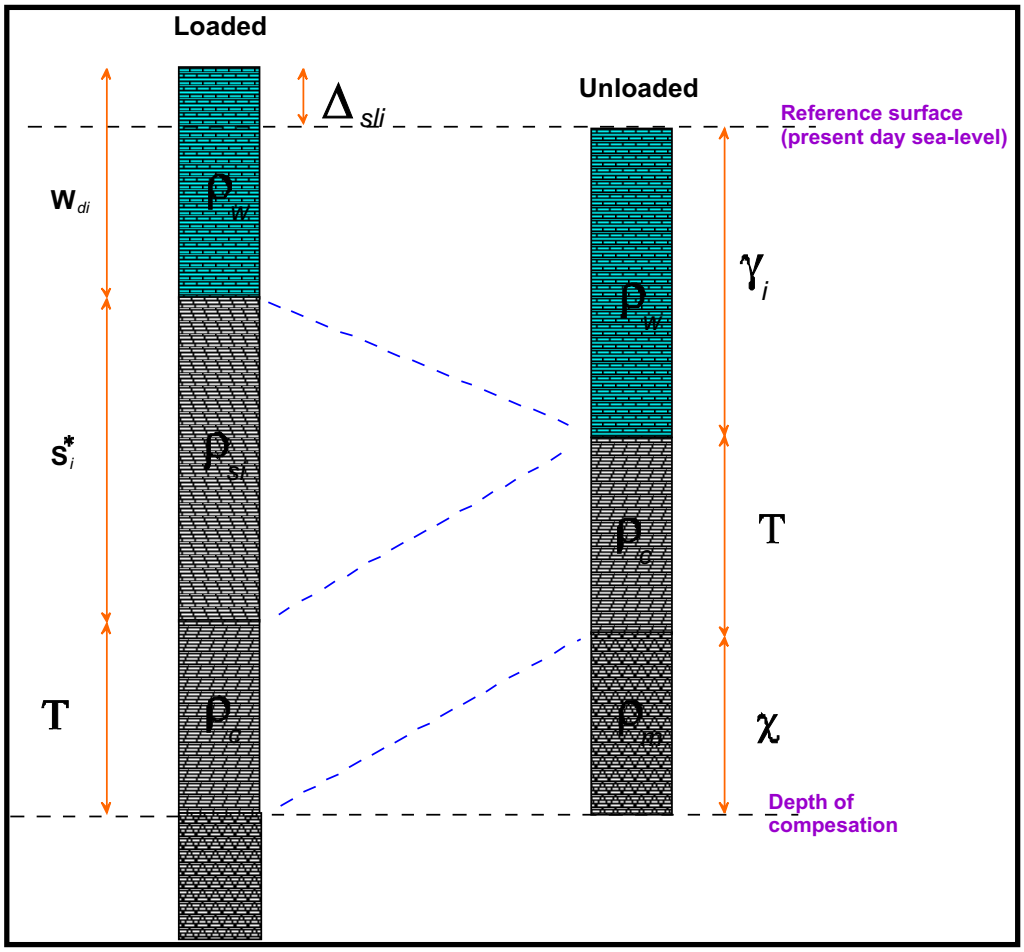

Fig. 4. Two columns of the crust and upper mantle before and after backstripping are in isostatic equilibrium (from Scalter and Christie, 1980).

De-compaction was considered as a mechanical, non-reversible process, where there was no alteration of the grains due to diagenesis. In that case we shall consider a cylinder of sediment and water schematically illustrated in Figure 5. The porosity of the sediment Φ is given by the ratio of the volume of water, V_w, to the total volume V_t. Assuming the cylinder is of uniform cross sectional area, Φ can be expressed as

$\Phi = h_w / h_t$ ---------- 4

where h_w and h_t are the heights of the water column and the total height of the column respectively. If h_g is the height of the sediment grains then

$h_t = h_w + h_g$ ---------- 5

Therefore $h_g = h_t (1 - \Phi)$ ---------- 6

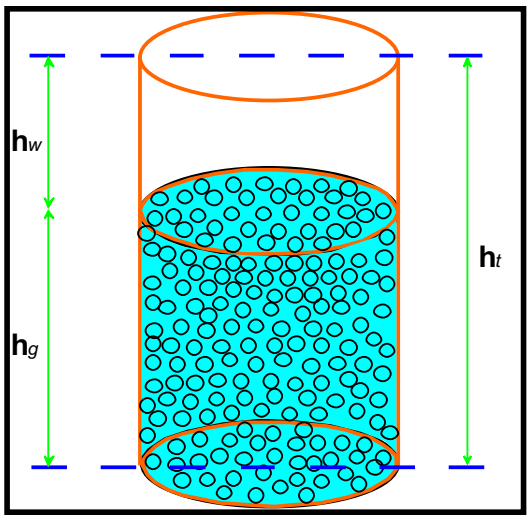

Fig. 5. Vertical cylinder showing height of water and sediment grains(http://atlas.geo.cornel.edu).

If we assume that during de-compaction (and compaction) h_g is constant and so as h_t changes so will Φ. Consider the i^{th} stratigraphic unit at some depth in a well which due to compaction has a thickness S_i and porosity Φ_i. The height of the grains is given by the equation

$h_g = S_i (1 - \Phi_i)$ ---------- 7

The height of the grains for the de-compacted unit is also h_g and so is given by

$h_g = S^*_i (1 - \Phi^*_i)$ ---------- 8

where S^*_i and Φ^*_i are the thickness and porosity of the de-compacted layer respectively (Fig. 6).

If we assume that the equivalent height of the grains is the same before and after compaction then we obtain the following by equating the two equations above:

$S^*_i = S_i (1 - \Phi_i) / (1 - \Phi^*_i)$ ---------- 9

This equation shows that the thickness of the de-compacted layer depends on the present day (i.e. compacted thickness) thickness and porosity, and the porosity when the unit was near the surface at the time of formation. Porosity values were estimated by "sliding" a unit up an approximate porosity versus depth curve of Bond and Kominz (1984) (Fig. 7). Present day thicknesses were determined from well logs.

The backstripping technique involves the unloading of a de-compacted sedimentary layer and so requires its thickness as well as an estimate of its density. This is most easily obtained by considering the volume and mass of the de-compacted layer. Therefore the following equations hold:

$V_t = V_w + V_g$ ---------- 10

$M_t = M_w + M_g$ ---------- 11

where t, w and g are the total, water and grain mass respectively, while V and M are for volume and mass. Solving for M in equation (11) , it then follows that:

$\rho_{si} V_t = \rho_w V_w + \rho_{gi} V_g$ ---------- 12

where ρ_{si} and ρ_{gi} are the average density and grain density of de-compacted layer, respectively. Substituting for V_g from equation (12) and dividing by V_t we get

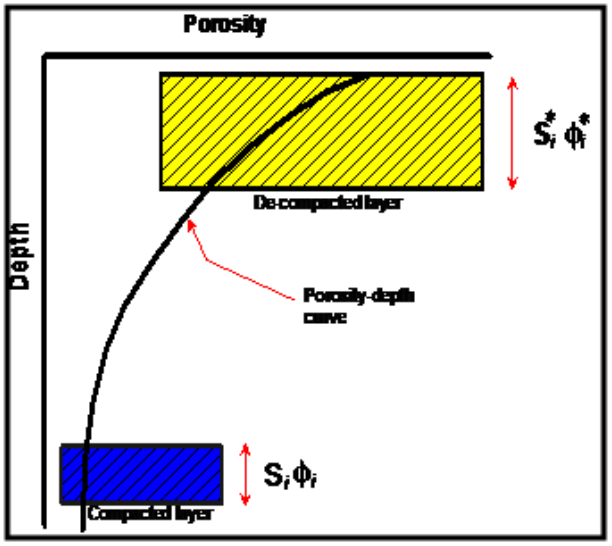

Fig. 6. Schematic diagram showing the thickness and porosity of a sedimentary layer at the surface and at depth (http://atlas.geo.cornel.edu).

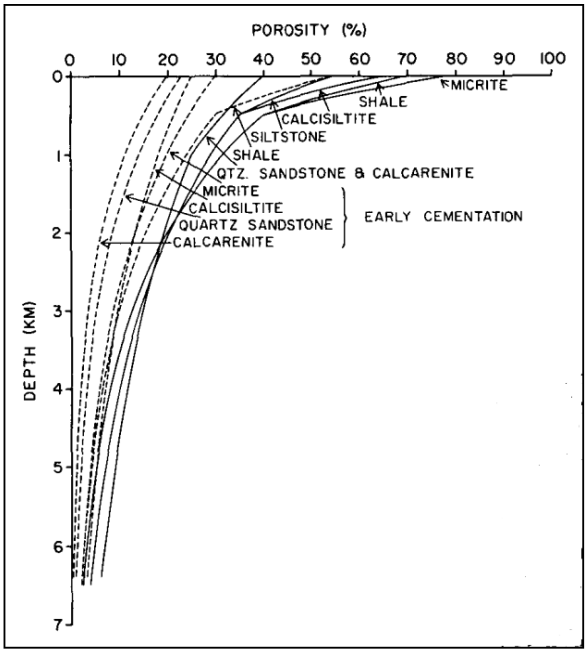

Fig.7. Summary of porosity vs depth curves for different lithologies from Bond and Kominz (1984).

$$\rho_{si} = \rho_w \Phi^*_i + \rho_{gi}(1-\Phi^*_i) \quad \text{---------- 13}$$

Equation 13 allows the density of decompacted layer to be calculated.

In the calculations carried out the following constants were used; density of mantle (ρ_m) = 3300 kgm^{-3}, density of sediment (ρ_{gi}) = 2720 kgm^{-3}, and density of water (ρ_w) = 1000 kgm^{-3}.

The procedure described above is only applicable in the backstripping of a single (i^{th}) sediment layer. In practice, backstripping affects more than one layer. To backstrip multiple layers restoration must be carried out for all the stratigraphic units in a sequence for each geologic time. That is, de-compacting the younger units and compacting the older ones (Fig. 8). The total thickness, S*, is easily obtained by summing all the individual thicknesses. In the case of the density, the mass of the total thickness must sum the masses of all the individual stratigraphic units within it and so we have that

$$\rho_s S^* = \sum_{i=1}^{n} \{ {}_{=ni1}\rho_w \Phi^*_i + \rho_{gi}(1-\Phi^*_i) \} S^*_i \gamma = \text{----- 14}$$

where n is the total number of stratigraphic units in the sequence at a particular time.

Therefore

$$\rho_s = \sum_{i=1}^{n} (\{\rho_w \Phi^*_i + \rho_{gi}(1-\Phi^*_i)\}\ S^*_i)/S^* \text{------ 15}$$

Finally, the total tectonic subsidence or uplift, γ, can then be obtained by substitution in the backstripping equation.

$$\gamma = W + S^* (\rho_m \rho)/(\rho_m \rho_w)\} - \Delta_{sl}\rho_m (\rho_m \rho_w) \quad \text{--------} \quad 16$$

where the first term in the equation is the water depth, the second a sediment loading term, and the third a sea-level loading term.

Water depth was determined from paleobathymetry data obtained from biostratigraphic information while relative sea level was determined from the sea level curve of Haq *et al.*, (1988). After all the parameters have been determined, they were input into Microsoft Excel package for computation.

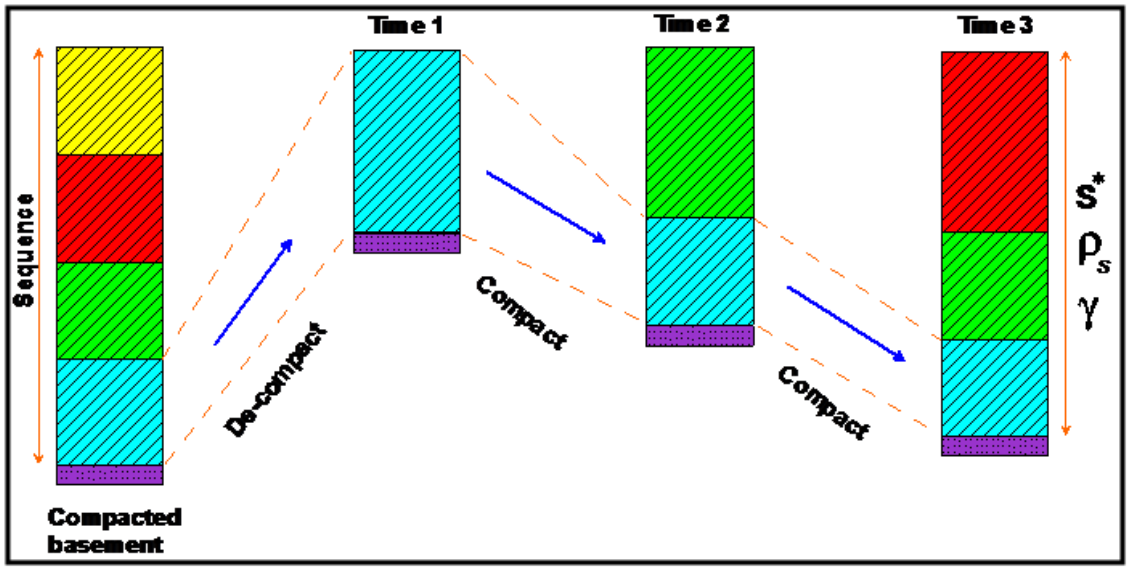

Fig. 8.Schematic diagram illustrating how multiple sediment layers can be backstripped (http://atlas.geo.cornel.edu).

RESULTS AND DISCUSSION

The thickness of the stratigraphic intervals, paleobathymetry and values obtained for the subsidence rates in the three wells are presented in Tables 1, 2 and 3. An attempt is made here to discuss some aspects of the evolution of the Benin Basin based on the data obtained from OML 97 for Upper Cretaceous and Tertiary times using the interplay of changing subsidence and sedimentation rates. The subsidence history of sedimentary basins is controlled by four main factors. These are: (a) changes in crustal thickness as a result of extension or shortening; (b) deposition or erosion, which results in loading or unloading of the crust; (c) changes in accommodation space and water loads as a result of local or global rise and fall in sea-level; and (d) density changes of the crust caused by thermal effects or some other processes such as magmatic underplating (Kusznir *et al.*, 1995; Watcharanantakul and Morley, 2000). From the subsidence analysis carried out on the three offshore wells, the following phases of tectonic subsidence may be identified in the tectonic and total subsidence history of the study area as shown in Figures 9, 10 and 11.

(a) Early late Cretaceous phase characterised by accelerated tectonic subsidence and gradual uplift patterns.
(b) Late Cretaceous phase characterised by relatively high uniform rates of subsidence and minor uplift.
(c) Paleogene to Neogene phase characterised by variable rates of tectonic subsidence and uplift.
(d) Quaternary phase starting with accelerated tectonic subsidence and followed by reduced rates of tectonic subsidence.

Three main episodes can be recognized in Epiya – 1, which penetrated Cenomanian to Santonian sediments. The first phase strictly occurred during Cenomanian and was characterised by period of subsidence followed by another period of zero vertical motion. This subsidence was approximately 81 m/Ma and was fully overbalanced by shallow marine to shelf sediments deposition of approximately 127 m/Ma. The next period

Table 1. Values obtained for the modeling of tectonic, sediment load and total subsidence in Baba 1.

Age	Lithology	Water	Mantle	Water Den	Grain Den	Constant	Depth poro	Sfc Poro	Lithified	RSL	Dcmpactd	SumDtpd	Avrg Dens	Dens	Dens/thick	Cum Dens	FinalDens	Ztect	LdSub	Ztotal
Upper Campanian	Sandstone	150	3300	1000	2720	1	0.05	0.22	106	250	129	129	2342	2634	302307	302307	2342	-155	75	-80
	Shale	150	3300	1000	2720	1	0.14	0.7	58	250	166	295	1516	2479	252060	554367	1877	-26	63	37
Maastrichtian	Sandstone	75	3300	1000	2720	1	0.055	0.22	24.4	195	30	325	2342	2625	69221	623588	1919	-10	12	2
	Shale	75	3300	1000	2720	1	0.145	0.7	23	240	66	390	1516	2471	99374	722962	1851	-23	24	1
	Sandstone	150	3300	1000	2720	1	0.057	0.18	19	190	22	412	2410	2622	52667	775629	1881	132	8	140
	Siltstone	150	3300	1000	2720	1	0.14	0.52	82	154	147	559	1826	2479	268211	1043840	1867	278	55	333
Lower Paleocene	Shale	150	3300	1000	2720	1	0.145	0.7	110	200	314	873	1516	2471	475266	1519106	1741	455	101	556
	Siltstone	150	3300	1000	2720	1	0.1	0.52	12	200	23	895	1826	2548	41076	1560182	1743	469	7	476
	Shale	150	3300	1000	2720	1	0.16	0.7	30.4	200	85	980	1516	2445	129042	1689224	1723	535	27	562
	Siltstone	150	3300	1000	2720	1	0.103	0.52	27	200	50	1031	1826	2543	92113	1781337	1728	568	16	584
	Shale	150	3300	1000	2720	1	0.165	0.7	30.4	200	85	1115	1516	2436	128274	1909611	1712	633	26	659
Upper Paleocene	Shale	150	3300	1000	2720	1	0.17	0.7	119	200	329	1445	1516	2428	499118	2408729	1667	889	96	984
	Siltstone	150	3300	1000	2720	1	0.17	0.52	15	180	26	1471	1826	2428	47352	2456080	1670	934	8	941
	Shale	150	3300	1000	2720	1	0.175	0.7	54	95	149	1619	1516	2419	225126	2681206	1656	1171	42	1213
	Siltstone	150	3300	1000	2720	1	0.18	0.52	15	210	26	1645	1826	2410	46781	2727987	1659	1022	7	1030
	Shale	350	3300	1000	2720	1	0.185	0.7	66	210	179	1824	1516	2402	271819	2999806	1645	1362	50	1412
Lower Miocene	Shale	350	3300	1000	2720	1	0.187	0.7	30	100	81	1905	1516	2398	123251	3123057	1639	1582	23	1605
	Siltstone	350	3300	1000	2720	1	0.185	0.52	32	110	54	1960	1826	2402	99191	3222248	1644	1603	15	1618
	Shale	150	3300	1000	2720	1	0.189	0.7	92	105	249	2208	1516	2395	377039	3599287	1630	1603	68	1671
Middle Miocene	Shale	350	3300	1000	2720	1	0.2	0.7	429	127	1144	3352	1516	2376	1734304	5333591	1591	2659	294	2953
Upper Miocene	Shale	350	3300	1000	2720	1	0.21	0.7	139	130	366	3718	1516	2359	554907	5888498	1584	2938	93	3031
	Sandstone	350	3300	1000	2720	1	0.099	0.22	22	20	25	3744	2342	2550	59507	5948004	1589	3107	7	3113
	Shale	350	3300	1000	2720	1	0.24	0.7	57	20	144	3888	1516	2307	218910	6166915	1586	3219	37	3256
Lower Pliocene	Shale	350	3300	1000	2720	1	0.25	0.7	262	50	655	4543	1516	2290	992980	7159895	1576	3684	164	3848
	Siltstone	150	3300	1000	2720	1	0.25	0.52	15	50	23	4567	1826	2290	42788	7202682	1577	3499	6	3505
	Shale	75	3300	1000	2720	1	0.27	0.7	85	50	207	4773	1516	2256	313559	7516241	1575	3584	52	3636
	Siltstone	75	3300	1000	2720	1	0.26	0.52	31	50	48	4821	1826	2273	87248	7603490	1577	3615	12	3627
	Shale	75	3300	1000	2720	1	0.28	0.7	101	-60	242	5064	1516	2238	367478	7970968	1574	3961	61	4021
Upper Pliocene	Sandstone	75	3300	1000	2720	1	0.14	0.22	82	-60	90	5154	2342	2479	211705	8182673	1588	3998	23	4022
	Shale	75	3300	1000	2720	1	0.302	0.7	27	-60	63	5217	1516	2201	95235	8277908	1587	4047	16	4063
	Sandstone	75	3300	1000	2720	1	0.125	0.22	21	-60	24	5240	2342	2505	55163	8333071	1590	4057	6	4063
	Shale	25	3300	1000	2720	1	0.32	0.7	73	-60	165	5406	1516	2170	250847	8583918	1588	4135	42	4178
	Sandstone	25	3300	1000	2720	1	0.145	0.22	21	-60	23	5429	2342	2471	53902	8637820	1591	4145	6	4151
	Shale	25	3300	1000	2720	1	0.325	0.7	30.4	-60	68	5497	1516	2161	103694	8741514	1590	4198	18	4215
	Sandstone	25	3300	1000	2720	1	0.146	0.22	12	-60	13	5510	2342	2469	30765	8772279	1592	4203	3	4207
	Shale	25	3300	1000	2720	1	0.326	0.7	37	5	83	5594	1516	2159	126020	8898299	1591	4175	21	4196
Quaternary	Sandstone	25	3300	1000	2720	1	0.147	0.22	40	5	44	5637	2342	2467	102430	9000729	1597	4193	11	4204
	Shale	25	3300	1000	2720	1	0.36	0.7	34	-60	73	5710	1516	2101	109961	9110690	1596	4342	19	4361
	Sandstone	25	3300	1000	2720	1	0.15	0.22	84	-60	92	5801	2342	2462	214346	9325036	1607	4381	24	4405
	Shale	25	3300	1000	2720	1	0.38	0.7	154	-60	318	6120	1516	2066	482492	9807529	1603	4627	83	4711
	Sandstone	25	3300	1000	2720	1	0.175	0.22	52	-60	55	6175	2342	2419	128788	9936317	1609	4650	15	4665
	Siltstone	25	3300	1000	2720	1	0.299	0.52	40	-60	58	6233	1826	2206	106645	10042962	1611	4688	16	4703
	Sandstone	25	3300	1000	2720	1	0.18	0.22	88	-60	93	6326	2342	2410	216628	10259590	1622	4726	25	4751
	Shale	25	3300	1000	2720	1	0.48	0.7	29	-60	50	6376	1516	1894	76204	10335794	1621	4765	14	4779
	Sandstone	25	3300	1000	2720	1	0.199	0.22	44	-60	45	6421	2342	2378	105804	10441599	1626	4784	12	4796
	Shale	25	3300	1000	2720	1	0.6	0.7	15	-60	20	6441	1516	1688	30320	10471919	1626	4800	5	4805
	Sandstone	25	3300	1000	2720	1	0.2	0.22	43	-60	44	6485	2342	2376	103271	10575189	1631	4818	12	4830
	Shale	25	3300	1000	2720	1	0.64	0.7	40	-60	48	6533	1516	1619	72768	10345651	1584	4987	12	4999
	Sandstone	25	3300	1000	2720	1	0.205	0.22	113	-60	115	6519	2342	2367	269689	10363280	1590	4959	30	4989

Table 2. Values obtained for the modelling of tectonic, sediment load and total subsidence in Epiya 1.

Age	Lithology	Water	Mantle	Water Den	Grain Den	Constant	Depth poro	Sfc Poro	Lithified	RSL	Dempactd	SumDrpd	Avrg Dens	Dens	Dens/thick	Cum Dens	FinalDens	Ztect	LdSub	Ztotal
Cenomanian	Shale	75	3300	1000	2720	1	0.14	0.7	32	270	92	92	1516	2479	139068	139068	1516	-241	21	-221
	Sandstone	75	3300	1000	2720	1	0.05	0.22	95	220	116	207	2342	2634	270935	410003	1977	-121	49	-72
	Shale	75	3300	1000	2720	1	0.15	0.7	82	234	232	440	1516	2462	352217	762220	1733	39	74	113
	Sandstone	75	3300	1000	2720	1	0.07	0.22	116	275	138	578	2342	2600	323861	1086081	1879	38	53	90
	Shale	75	3300	1000	2720	1	0.17	0.7	70	110	194	772	1516	2428	293599	1379680	1788	425	66	491
Turonian	Siltstone	150	3300	1000	2720	1	0.12	0.52	79	110	145	917	1826	2514	264408	1644088	1794	592	50	642
	Shale	150	3300	1000	2720	1	0.175	0.22	129	110	136	1053	2342	2419	319493	1963581	1865	649	51	701
Coniacian	Shale	150	3300	1000	2720	1	0.18	0.7	18	110	49	1102	1516	2410	74587	2038168	1849	687	18	706
Santonian	Shale	150	3300	1000	2720	1	0.18	0.7	12	200	33	1135	1516	2410	49725	2087893	1840	584	12	596
Campanian	Shale	50	3300	1000	2720	1	0.18	0.7	64	250	175	1310	1516	2410	265199	2353092	1796	548	61	608
Early Maastrichtian	Sandstone	50	3300	1000	2720	1	0.08	0.22	12	195	14	1324	2342	2582	33143	2386235	1802	633	5	637
	Shale	50	3300	1000	2720	1	0.19	0.7	101	240	273	1597	1516	2393	413413	2799648	1753	779	89	869
	Siltstone	50	3300	1000	2720	1	0.14	0.5	46	190	79	1676	1860	2479	147163	2946811	1758	901	26	927
	Shale	50	3300	1000	2720	1	0.2	0.7	15	154	40	1716	1516	2376	60640	3007451	1753	983	13	997
Paleocene	Sandstone	75	3300	1000	2720	1	0.09	0.22	15	200	18	1733	2342	2565	40978	3048429	1759	950	6	956
	Shale	75	3300	1000	2720	1	0.18	0.7	15	200	41	1774	1516	2410	62156	3110585	1753	982	13	995
	Siltstone	75	3300	1000	2720	1	0.15	0.52	34	200	60	1835	1826	2462	109916	3220502	1755	1020	20	1040
	Shale	75	3300	1000	2720	1	0.19	0.7	30	180	81	1916	1516	2393	122796	3343298	1745	1112	26	1138
	Siltstone	75	3300	1000	2720	1	0.16	0.52	24	95	42	1958	1826	2445	76675	3419973	1747	1261	14	1274
	Shale	75	3300	1000	2720	1	0.2	0.7	302	95	805	2763	1516	2376	1220885	4640858	1680	1885	238	2123
Eocene	Shale	75	3300	1000	2720	1	0.24	0.7	12	210	30	2793	1516	2307	46086	4686944	1678	1744	9	1753
	Siltstone	75	3300	1000	2720	1	0.19	0.52	12	210	20	2814	1826	2393	36968	4723913	1679	1757	6	1763
	Sandstone	75	3300	1000	2720	1	0.11	0.22	24	99	27	2841	2342	2531	64124	4788037	1685	1927	8	1936
	Shale	75	3300	1000	2720	1	0.25	0.7	37	150	93	2934	1516	2290	140230	4928267	1680	1926	27	1953
	Sandstone	75	3300	1000	2720	1	0.12	0.22	9	100	10	2944	2342	2514	23776	4952043	1682	2002	3	2005
	Shale	75	3300	1000	2720	1	0.26	0.7	15	100	37	2981	1516	2273	56092	5008135	1680	2031	11	2042
Oligocene	Shale	75	3300	1000	2720	1	0.26	0.7	110	110	271	3252	1516	2273	411341	5419476	1667	2227	79	2305
Early Miocene	Shale	25	3300	1000	2720	1	0.27	0.7	189	110	460	3712	1516	2256	697208	6116685	1648	2534	130	2663
	Sandstone	25	3300	1000	2720	1	0.13	0.22	46	105	51	3763	2342	2496	120142	6236827	1657	2562	15	2577
	Shale	75	3300	1000	2720	1	0.28	0.7	46	96	110	3874	1516	2238	167366	6404193	1653	2711	31	2742
	Sandstone	75	3300	1000	2720	1	0.14	0.22	76	130	84	3957	2342	2479	196214	6600407	1668	2697	24	2721
	Shale	150	3300	1000	2720	1	0.3	0.7	18	140	42	3999	1516	2204	63672	6664079	1666	2790	12	2802
	Sandstone	150	3300	1000	2720	1	0.15	0.22	18	135	20	4019	2342	2462	45931	6710011	1670	2805	6	2811
	Shale	150	3300	1000	2720	1	0.31	0.7	210	50	483	4502	1516	2187	732228	7442239	1653	3302	137	3439
Middle Miocene	Shale	150	3300	1000	2720	1	0.33	0.7	54	150	121	4623	1516	2152	182830	7625068	1650	3252	34	3286
	Siltstone	150	3300	1000	2720	1	0.25	0.52	9	105	14	4637	1826	2290	25673	7650741	1650	3326	4	3330
	Shale	150	3300	1000	2720	1	0.36	0.7	104	130	222	4859	1516	2101	336350	7987091	1644	3462	62	3524
Late Miocene	Shale	150	3300	1000	2720	1	0.37	0.7	128	50	269	5127	1516	2084	407501	8394591	1637	3785	74	3860
Early Pliocene	Shale	75	3300	1000	2720	1	0.37	0.7	122	70	256	5384	1516	2084	388399	8782991	1631	3880	70	3950
	Sandstone	75	3300	1000	2720	1	0.18	0.22	18	70	19	5402	2342	2410	44310	8827301	1634	3888	5	3893
	Shale	75	3300	1000	2720	1	0.43	0.7	24	70	46	5448	1516	1980	69130	8896430	1633	3923	13	3936
	Sandstone	75	3300	1000	2720	1	0.18	0.22	6	70	6	5454	2342	2410	14770	8911201	1634	3926	2	3928
	Shale	75	3300	1000	2720	1	0.45	0.7	9	70	17	5471	1516	1946	25014	8936215	1633	3939	5	3943
	Sandstone	75	3300	1000	2720	1	0.19	0.22	9	70	9	5480	2342	2393	21885	8958099	1635	3943	3	3945
	Shale	75	3300	1000	2720	1	0.49	0.7	146	70	248	5728	1516	1877	376271	9334371	1629	4135	68	4203
	Sandstone	75	3300	1000	2720	1	0.2	0.22	94	70	96	5825	2342	2376	225754	9560125	1641	4175	27	4202
	Shale	75	3300	1000	2720	1	0.5	0.7	6	70	10	5835	1516	1860	15160	9575285	1641	4183	3	4186
	Sandstone	75	3300	1000	2720	1	0.2	0.22	6	70	6	5841	2342	2376	14410	9450627	1618	4246	2	4248

Table3.Values obtained for the modelling of tectonic, sediment load and total subsidence in Ayetoro 1.

Age	Lithology	Water	Mantle	Water Den	Grain Den	Constant	Depth poro	Sfc Poro	Lithified	RSL	Decompacted	SumDtpd	Avg Dens	Dens	Dens/thick	Cum Dens	FinalDens	Zmectonics	LoadSub	Ztotal
Upper Campanian	Sandstone	25	3300	1000	2720	1	0.04	0.22	146	17	180	180	2342	2651.2	4207667.5	4207667.5	2341.6	75.5	104.8	180.3
Maastrichian	Sandstone	150	3300	1000	2720	1	0.04	0.22	25	17	31	210	2342	2651.2	72049.2	4928816.7	2341.6	213.3	17.9	231.3
		75	3300	1000	2720	1	0.04	0.22	42	17	52	262	2342	2651.2	1210422.7	6138859.4	2341.6	159.8	30.2	190.0
	Lam Shale	150	3300	1000	2720	1	0.13	0.7	75	17	218	480	1516	2496.4	329730.0	943589.4	1967.2	403.6	91.5	495.0
	Lam Shale	75	3300	1000	2720	1	0.13	0.7	33	17	96	575	1516	2496.4	145081.2	10886716	1892.2	402.8	37.1	439.9
Lower Paleocene	Shale	150	3300	1000	2720	1	0.14	0.7	81	70	232	808	1516	2479.2	352015.2	14406685.8	1784.0	581.8	79.2	661.0
	Siltstone	150	3300	1000	2720	1	0.1	0.52	7	70	13	821	1826	2548.0	23961.0	14646646.8	1784.7	590.3	4.5	594.7
	Siltstone	75	3300	1000	2720	1	0.1	0.52	27	70	51	871	1826	2548.0	92421.0	15570967.8	1787.1	547.7	17.3	565.0
Upper Paleocene	Siltstone	150	3300	1000	2720	1	0.15	0.42	57	70	84	955	1998	2462.0	1668685.5	17239936.3	1805.5	670.0	29.3	699.3
	Sandstone	150	3300	1000	2720	1	0.06	0.22	56	122	67	1022	2342	2616.8	1580284.0	18819064.3	1840.9	623.5	24.7	648.2
	Shale	150	3300	1000	2720	1	0.15	0.7	33	122	94	1116	1516	2462.0	1417746.0	20237110.3	1813.6	696.0	33.1	729.1
Eocene	Sandstone	150	3300	1000	2720	1	0.06	0.22	24	20	29	1145	2342	2616.8	67726.3	20091436.6	1827.0	854.4	10.4	864.8
	Sandstone	350	3300	1000	2720	1	0.06	0.22	13	20	16	1160	2342	2616.8	36685.1	21281217	1833.9	1061.0	5.7	1066.7
	Siltstone	350	3300	1000	2720	1	0.12	0.52	48	20	88	1248	1826	2513.6	160652.8	22587745	1833.3	1117.4	31.9	1149.3
Lower Miocene	Siltstone	350	3300	1000	2720	1	0.123	0.52	13	73	24	1272	1826	2508.4	43361.8	23321363	1833.2	1056.6	8.6	1065.2
	Siltstone	150	3300	1000	2720	1	0.125	0.52	24	73	44	1316	1826	2505.0	79870.0	24120063	1832.9	884.6	15.8	900.5
	Shale	150	3300	1000	2720	1	0.17	0.7	61	73	169	1485	1516	2427.6	255850.3	26678565	1796.9	1015.5	58.5	1074.0
	Sandstone	150	3300	1000	2720	1	0.065	0.22	12	71	14	1499	2342	2608.2	33683.0	27015395	1802.1	1024.4	5.0	1029.4
	Sandstone	350	3300	1000	2720	1	0.067	0.22	3	71	4	1503	2342	2604.8	8402.7	27099423	1803.4	1225.9	1.3	1227.1
Middle Miocene	Lam Shale	350	3300	1000	2720	1	0.17	0.7	21	100	58	1561	1516	2427.6	88079.6	27982021.9	1792.7	1229.3	20.0	1249.4
	Lam Shale	150	3300	1000	2720	1	0.173	0.7	123	100	339	1900	1516	2422.4	514030.1	33120352.0	1743.3	1292.3	109.6	1401.9
	Lam Shale	350	3300	1000	2720	1	0.175	0.7	25	100	69	1969	1516	2419.0	104225.0	34162277.0	1735.4	1545.7	22.0	1567.6
	Lam Shale	150	3300	1000	2720	1	0.178	0.7	30	100	82	2051	1516	2413.8	1246615.2	35408892.2	1726.6	1409.4	26.0	1435.4
	Shale	150	3300	1000	2720	1	0.18	0.7	76	100	208	2259	1516	2410.4	3149323.7	38558815.9	1707.2	1570.6	63.9	1634.4
	Siltstone	150	3300	1000	2720	1	0.13	0.52	15	100	27	2286	1826	2496.4	49633.5	39054049.4	1708.6	1588.0	8.4	1596.4
	Siltstone	350	3300	1000	2720	1	0.135	0.52	98	100	177	2462	1826	2487.8	322408.6	42278858.0	1717.0	1901.2	55.1	1956.2
Upper Miocene	Siltstone	175	3300	1000	2720	1	0.14	0.52	24	40	43	2505	1826	2479.2	78500.8	43106358.8	1718.9	1839.8	13.4	1853.3
	Siltstone	125	3300	1000	2720	1	0.142	0.52	16	40	29	2534	1826	2475.8	52212.2	43585871.0	1720.1	1808.2	9.0	1817.1
	Shale	125	3300	1000	2720	1	0.19	0.7	25	40	68	2601	1516	2393.2	1023300	44609901.0	1714.8	1860.5	21.0	1881.5
	Shale	150	3300	1000	2720	1	0.193	0.7	5	40	13	2615	1516	2388.0	20390.2	44812912	1713.8	1896.0	4.2	1900.1
	Shale	150	3300	1000	2720	1	0.198	0.7	52	40	139	2754	1516	2379.4	210744.2	46920354	1703.8	2003.8	42.5	2046.3
Pliocene	Shale	150	3300	1000	2720	1	0.2	0.7	31	75	83	2837	1516	2376.0	1253227	48173580	1698.3	2017.7	25.1	2042.8
	Shale	25	3300	1000	2720	1	0.21	0.7	296	75	779	3616	1516	2358.8	11816715	59990029.5	1659.0	2497.3	223.3	2720.6
	Siltstone	25	3300	1000	2720	1	0.16	0.52	46	75	81	3696	1826	2444.8	1469060.8	61459990.3	1662.7	2548.9	23.2	2572.1
Pleistocene	Siltstone	25	3300	1000	2720	1	0.17	0.52	38	5	66	3762	1826	2427.6	1199571	62659474	1665.5	2691.5	19.0	2710.5
	Shale	25	3300	1000	2720	1	0.215	0.7	27	5	71	3833	1516	2350.2	1071054	63730528	1662.7	2746.3	20.4	2766.6
	Siltstone	25	3300	1000	2720	1	0.173	0.52	80	5	138	3971	1826	2422.4	2516028.5	66246814	1668.4	2834.6	40.1	2874.7
	Sandstone	25	3300	1000	2720	1	0.075	0.22	53	5	63	4034	2342	2591.0	1471756.6	67718569	1678.9	2863.0	18.6	2881.5
	Shale	25	3300	1000	2720	1	0.24	0.7	75	5	190	4224	1516	2307.2	2880400	70598969	1671.6	3010.3	55.5	3065.8
	Sandstone	25	3300	1000	2720	1	0.08	0.22	70	5	83	4306	2342	2582.4	1933321	72532290	1684.4	3044.7	24.6	3069.3
	Siltstone	25	3300	1000	2720	1	0.19	0.52	98	5	165	4471	1826	2393.2	3019086	75551376	1689.6	3150.8	49.6	3200.3
	Shale	25	3300	1000	2720	1	0.25	0.7	77	5	193	4664	1516	2290.0	2918300	78469676	1682.5	3300.1	57.1	3357.2
	Sandstone	25	3300	1000	2720	1	0.085	0.22	23	5	27	4691	2342	2573.8	63178.2	79101453	1686.3	3311.3	8.1	3319.4
	Shale	25	3300	1000	2720	1	0.29	0.7	31	5	73	4764	1516	2221.2	1112239	80213693.7	1683.6	3368.2	21.8	3390.0
	Sandstone	25	3300	1000	2720	1	0.14	0.22	26	5	29	4793	2342	2479.2	67125.9	80884495.5	1687.6	3380.2	8.6	3388.7
	Shale	25	3300	1000	2720	1	0.3	0.7	65	5	152	4945	1516	2204.0	2299267	83184222.2	1682.3	3497.8	45.0	3542.8
	Sandstone	25	3300	1000	2720	1	0.145	0.22	44	5	48	4993	2342	2470.6	1123937.2	84313594.4	1688.7	3517.9	14.4	3532.3
	Shale	25	3300	1000	2720	1	0.32	0.7	24	5	54	5047	1516	2169.6	824704	85138298	1686.8	3560.1	16.2	3576.3
	Sandstone	25	3300	1000	2720	1	0.15	0.22	34	5	37	5084	2342	2462.0	86750.3	86005891	1691.6	3575.5	11.1	3586.7
	Sandstone	75	3300	1000	2720	1	0.155	0.22	36	5	39	5123	2342	2453.4	91322.4	86091911.5	1696.5	3641.8	11.8	3653.6
	Sandstone	25	3300	1000	2720	1	0.158	0.22	3	5	3	5127	2342	2448.2	7583.2	86094494.6	1696.9	3593.1	1.0	3594.1

of subsidence cut across both Cenomanian and Turonian ages. During this period, subsidence rate increased to 91.9 m/Ma. There was probably no significant change in the environments of deposition of the sediments. However sedimentation rate during these ages averaged

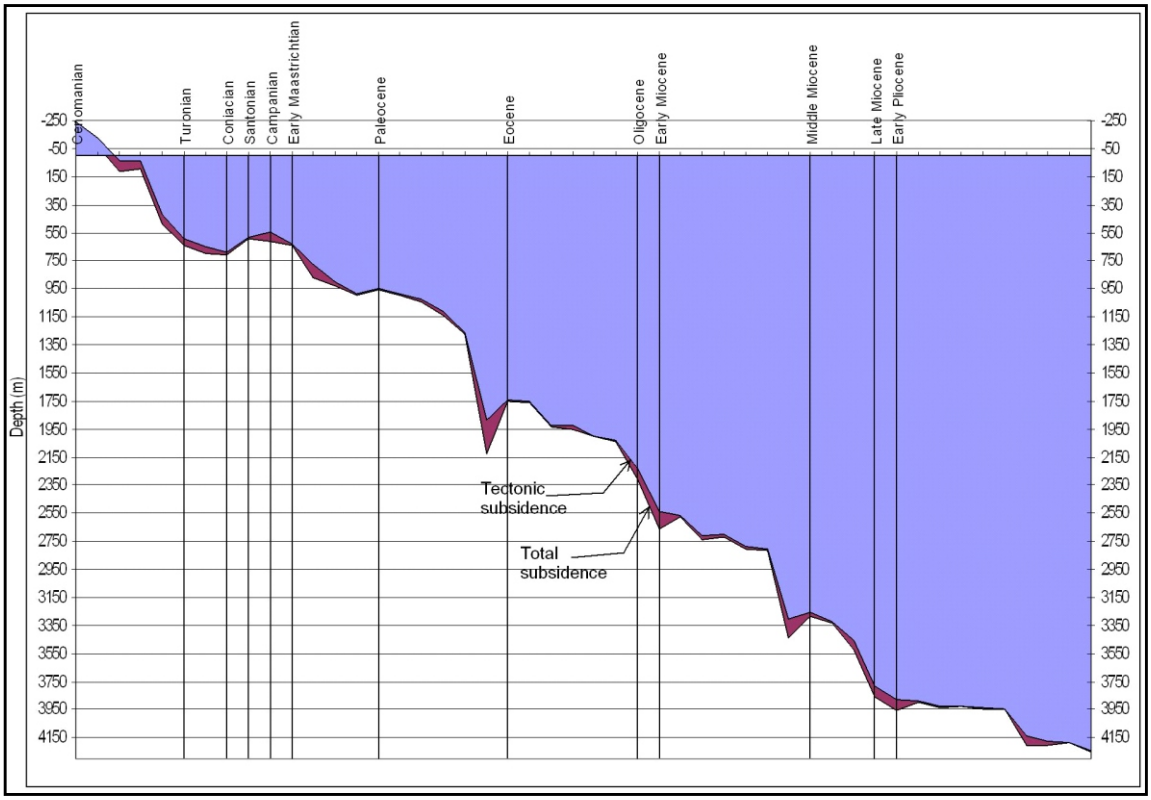

Fig. 9. Subsidence and uplift patterns in Epiya – 1 well.

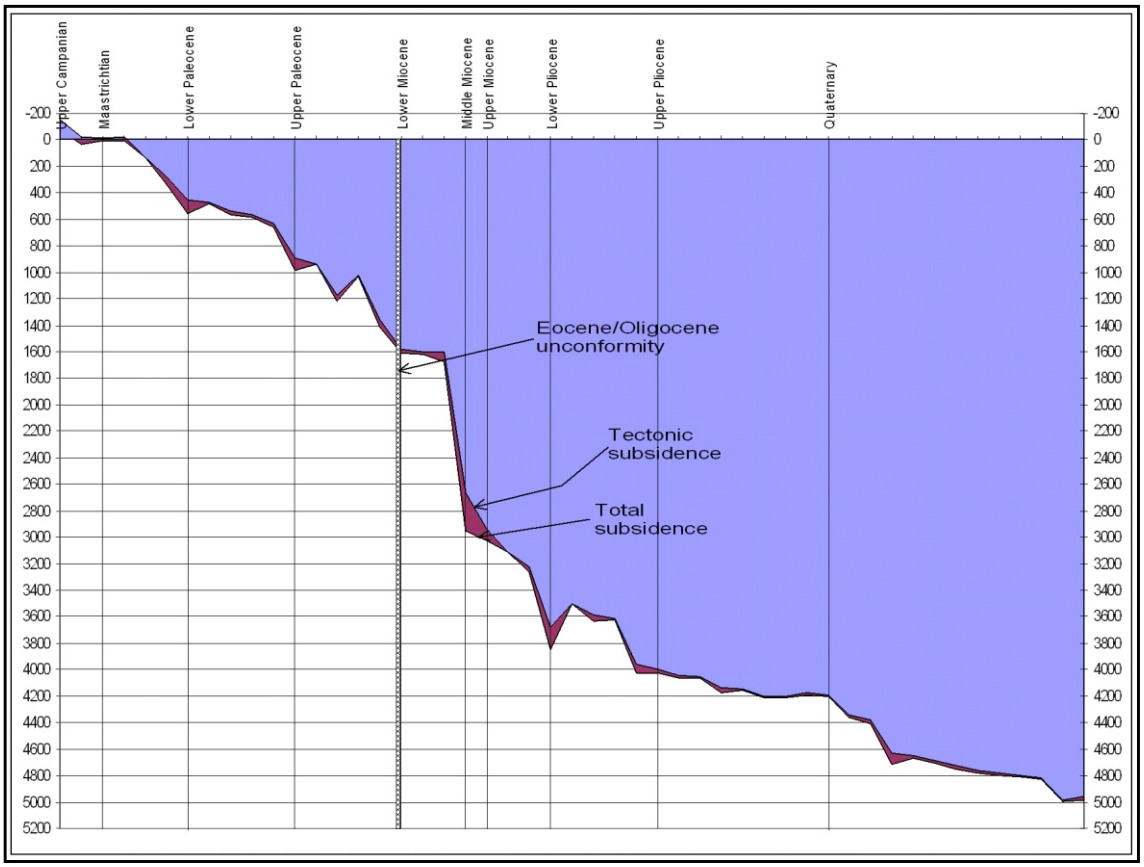

Fig. 10. Model showing subsidence and uplift patterns in Baba – 1 well.

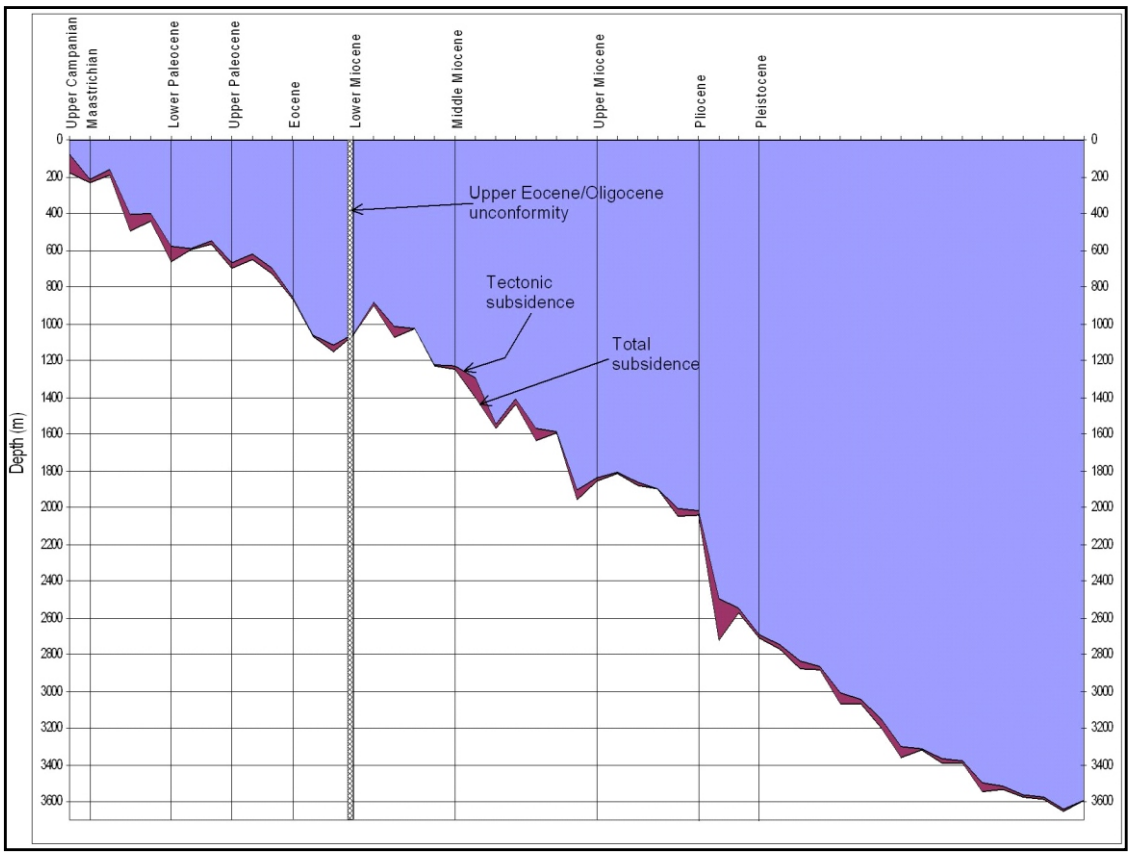

Fig. 11. Subsidence patterns in Ayetoro – 1 well. Periods of unconformity and uplift are shown in the model.

approximately 97 m/Ma. The Coniacian through Santonian were periods characterised by uplift at slow rate of 31 m/Ma. This was balanced by very slow rate of sedimentation at a rate that averaged 13 m/Ma for these geological ages. This slow rate of uplift combined with slow rate of sedimentation was probably responsible for the Santonian regression experienced in this part of the basin.

At the expiration of the uplift during late Santonian another period of subsidence started in Campanian, which marked the onset of sedimentation in the location of Baba – 1 and Ayetoro – 1 wells. This period of subsidence was investigated in three wells - Baba – 1, Ayetoro – 1 and Epiya – 1. The subsidence probably took place at a very slow rate not higher than 10m/M in Baba – 1, and Ayetoro – 1 wells. Sedimentation rate during this period was equally slow; it varied from 14 m/Ma to 23 m/Ma as indicated in the wells.

As evidenced in the wells, the Maastrichtian age experienced an unsteady tectonic event characterised by different periods of subsidence and uplift observed in the three wells. The tectonic evolution of the basin as documented in Baba – 1 and Epiya – 1 involved subsidence at the rate of 141.1 m/Ma to 26.9 m/Ma. As shown in Epiya – 1, this slow subsidence rate began in the Campanian and terminated before the end of Maastrichtian. Subsequently a period of no vertical motion took place for about 1.2 Ma and this terminated at the end of Maastrichtian. Analysis performed on Ayetoro – 1 showed that there were two periods of tectonic uplift (57.6 m/Ma and 28.8 m/Ma) and two periods of subsidence (208.6 m/Ma and 143.9 m/Ma). This inconsistent tectonic events was fully balanced by moderate sedimentation rates of 80 m/Ma, 78 m/Ma and 52 m/Ma as documented in Epiya – 1, Ayetoro – 1 and Baba – 1, respectively. This complex pattern of motions, especially the periods of uplift and moderate rate of sedimentation were probably responsible for the shallowing of the sediments and erosion that took place in upper Maastrichtian.

The Paleocene age also represents another period of variable tectonic movements. Information obtained from Ayetoto – 1 and Baba – 1 shows that uplift conditions started at the beginning of Early Paleocene at a rate higher in Baba – 1 (57.7 m/Ma) and slower in Ayetoro – 1 (21.6 m/Ma). Subsequently, it was accompanied by subsidence which initially was slower in Baba – 1 (48.1 m/Ma) and suddenly increased to 351 m/Ma for a short period of 1.04 Ma. The Upper Paleocene age in the location of Baba – 1 was characterised by alternating two periods of uplift and subsidence. The first and second periods of uplift occur at 77.8 m/Ma and 188.9 m/Ma, respectively while the first and second subsidence took place at high rate of 305 m/Ma and 283.3 m/Ma, respectively. As shown in Ayetoro – 1, Upper Paleocene tectonic activities equally began with a period of uplift (21.6 m/Ma) accompanied by moderate subsidence (74.1 m/Ma), which extended to and terminated in the Eocene. Tectonic activities as documented in Epiya – 1 during the Paleocene differ slightly from those documented in the other two wells, which consists of two periods of continuous differing subsidence rates and one period of uplift. In addition, these events could not be differentiated from those of Early and Lower Paleocene owing to poor resolution of data. The Paleocene period began with a slow rate of subsidence (49.5 m/Ma) and suddenly increased to 740.1 m/Ma. A similar scenario was observed in Baba – 1 as explained above. After the cessation of the subsidence, there was another period characterised by high rate of uplift (309.8 m/Ma). This uplift terminated the Paleocene tectonic events as recorded in Epiya – 1. Sedimentation rate was high in Epiya – 1 (108 m/Ma) and diminished from the Early Paleocene (Baba – 1, 57 m/Ma; Ayetoro -1. 31 m/Ma) to Late Paleocene (Baba – 1.32 m/Ma; Ayetoro -1. 11 m/Ma) in the other two wells. This rate of sedimentation probably could not keep pace with the high rate of subsidence leading to deepening trend of facies. However, the relatively high rate of uplift recorded in the Late Paleocene was probably caused subsequent erosion that prevented the preservation of Eocene and Oligocene sediments.

Eocene and Oligocene tectonic events were not documented in Baba – 1 and Ayetoro – 1, because of poor to non-preservation of these sediments in these two wells. Eocene sediments were poorly preserved in Ayetoro – 1 with uncompacted sediment thickness totalling 132.6 m and there was no documentation of such sediments in Baba – 1. However, these sediments were preserved in Epiya – 1, which enabled the determination of tectonic events during these geological ages.

The Eocene to Oligocene tectonic evolution was characterised by three main episodes; two are restricted to the Eocene while the last episode began in Late Eocene and lasted till the end of Oligocene. The first phase exhibited moderate subsidence at the rate of 24.7 m/Ma. This phase was followed by period of decreased subsidence with a rate (9.1 m/Ma) that was less than half of the first phase. The following phase, which extended to the Oligocene experienced relatively rapid subsidence and attained a rate of 41.3 m/Ma. Sediment input was very low during Eocene to Oligocene as documented in Epiya – 1. There was sharp decrease in the rate of sedimentation from 108 m/Ma in Paleocene to 10m/Ma in Eocene, which gradually increased to 25 m/Ma during Oligocene. The Eocene to Oligocene subsidence was fully compensated for by the deposition of marine mid shelf sediments, with progressive upward shallowing. This caused periodic fluvio-marine conditions in the later part of the sedimentation. Low sedimentation rates and upward shallowing of the sediments could have been caused by the previous high rate of uplift recorded in Late Paleocene. Available evidence from seismic showed that erosion has affected some parts of the area, especially the locations of Baba – 1 and Ayetoro – 1, during the Eocene and Oligocene. This erosion did not affect the location of Epiya – 1. This suggests significant difference in the rate of uplift in the area.

Uplift was documented in two wells at the beginning of Miocene at the rate of 79.2 m/Ma and 43.6 m/Ma in Epiya – 1 and Ayetoro – 1 respectively. Subsequently, two phases of subsidence was preserved in Epiya – 1 at a rate of 52 m/Ma and 594.1 m/Ma. This corresponds to increasing rate of subsidence. A period of uplift at a rate of 59.4 m/Ma ended the tectonic event in the area of Epiya – 1 well during Early

Miocene. In a similar manner, subsidence followed the initial uplift in the location of Ayetoro – 1 at an high rate of 113.3 m/Ma. Contrary to the event recorded in Epiya – 1 this was followed by slow rate (35.4 m/Ma) of uplift, while another high rate of subsidence (141.6 m/Ma) followed this uplift and terminated the Early Miocene tectonic event in the location of Ayetoro – 1. The irregular nature of tectonic event recoded in the previous two wells during Early Miocene was not present in Baba – 1. Two episodes were recorded, the first phase was characterised by very low subsidence rate (4.2 m/Ma). Subsequently, it was replaced by an high rate of subsidence (586.5 m/Ma). The Early Miocene sedimentary succession began to be deposited in marine outer shelf environment characterised by fluvio-marine influence similar to the Oligocene. Sedimentation rates were not uniform in the three wells, Epiya – 1 was characterised by high rate (177 m/Ma) compared with Baba – 1 and Ayetoro – 1 areas that received 35 m/Ma and 36 m/Ma, respectively. This non-uniformity in the amount of sediment received in the different locations of the wells was probably related to different amount of sediments supplied to these locations. In addition, the increasing and extremely high subsidence rate (594.1 m/Ma) experienced in Eipya – 1 for long period (5.05 Ma) may account for the high rate of sediment deposition when compared with those of the locations in other two wells.

Subsidence pattern in the Middle Miocene was almost similar in Epiya – 1 and Baba – 1, when only one phase of subsidence was recorded. In Epiya – 1, the subsidence started at a moderate rate and attained a high rate of 126.1 m/Ma within a period of 4.4 Ma and terminated at the beginning of Upper Miocene. In Baba – 1, the subsidence began during Middle Miocene and ran through the earliest part of Upper Miocene. The rate was low (31.6 m/Ma) and occurred within a longer period of 8.5 Ma, when compared with the rate at Epiya – 1. The pattern of subsidence in Ayetoro – 1 is different from those of Baba – 1 and Epiya – 1. Three episodes of subsidence and uplift were documented in the well. The first phase of subsidence occurred at very high rate of 274.2 m/Ma within a time interval of 1.24 Ma. This was accompanied by ephemeral uplift that took place within 0.62 Ma at a rate of 258.1 m/Ma. This represents a very high rate of uplift when compared with the previous ones, but the time interval was of short duration. Similarly another period of ephemeral subsidence followed this uplift at a very high rate of 306.5 m/Ma. The following uplift was at a rate of 230.2 m/Ma. Lastly there was another ephemeral subsidence that has the highest rate (612.9 m/Ma) within the interval. The Middle Miocene sedimentary succession was deposited in deep marine environments ranging from outer neritic to bathyal environment in all the locations of the three wells. However, sedimentation rates were higher in Baba – 1 and Ayetoro – 1 with the two wells having values of 162 m/Ma and 220 m/Ma, respectively. Epiya – 1 was characterised by low rate of 82 m/Ma within an interval of 4.4 Ma. The increased rate of sedimentation observed in Baba – 1 and Ayetoro – 1 was probably related to extremely high rate of subsidence documented during this period. Although high rate of subsidence was not recorded in Baba – 1, it will be recalled that upper Lower Miocene (preceding Middle Miocene) in Baba – 1 recorded an unprecedented amount of subsidence rate (586.5 m/Ma). This high rate of subsidence was interpreted as being responsible for the high rate of sediment accumulation.

Low subsidence rate (12.7 m/Ma) with one phase characterised Late Miocene in Epiya – 1, whereas the situation was not the same in Baba – 1 where two episodes of subsidence were recorded with the initial one extending from Middle Miocene to Late Miocene at a low rate of 31.6 m/Ma. This phase was accompanied by fast subsidence phase (about 267.9 m/Ma). The accelerated subsidence phase terminated at the end Late Miocene. In Ayetoro – 1, the situation is different from the two described above. The uplift that ended the tectonic activity during Middle Miocene extended to the beginning of Late Miocene. It occurred within a period of 1.25 Ma at a rate of 88 m/Ma. Subsequently, this uplift was replaced by moderate subsidence at a rate of 57.1 m/Ma. The last period that lasted for about 2.5 Ma experienced no vertical motion; hence uplift or subsidence was not recorded. The variable pattern of tectonic activities experienced in the three wells was fully compensated for by deposition in marine environments possibly

restricted to outer neritic environment in all the locations of the wells. Sedimentation rate decreased in Epiya – 1 from the previous 177 m/Ma to 82 m/Ma, contrary to the case of Baba – 1 that experienced increase in sedimentation rate from 162 m/Ma to 442 m/Ma. Also sharp decrease was observed in Ayetoro – 1, where the rate of sedimentation decreased from 220 m/Ma to 46 m/Ma. The increased rate of sedimentation observed in Baba – 1 compared with the other two wells was interpreted as the high rate of subsidence documented in the well.

Tectonic evolution for Pliocene section was well documented in Baba – 1. The sediments were classified as Early and Late Pliocene owing to the resolution of data in the well. The Lower Pliocene section in Baba – 1 is typically composed of four episodes of tectonic activities, and the fifth episode extended to Late Pliocece. The first phase is characterised by upward motion (uplift) at a very high rate of 750 m/Ma. This uplift probably took place within a short geological period of 0.34 Ma. This was followed by a period of another subsidence that occurred at a rate of 173 m/Ma. Subsequently, there was a short period of basin quiescence when there was no vertical motion. This period lasted for 0.35 Ma approximately. An unprecedented high rate of subsidence accompanied the period of basin quiescence. During this period the subsidence rate rose to 1183.6 m/Ma within a short interval of 0.35 Ma. The fifth episode of subsidence extended to Late Pliocene and was characterised by slow rate of 75 m/Ma. During the period, vertical motion of the basin in the location of Baba – 1 was not as significant as that of Early Pliocene. The accompanying period of basin subsidence occurred at a rate of 491 m/Ma within an interval of 0.22 Ma. There was no vertical motion recorded in the well in the later part of Late Pliocene for another period of 0.66 Ma until the beginning of Quaternary.

In the location of Epiya – 1, Pliocene local tectonic event is composed of a period of uplift, two periods of quiescence and two periods of subsidence. It started with an uplift at a rate of 129 m/Ma followed by another period of subsidence at a rate of 102 m/Ma. Each of them lasted for an estimated period of 0.39 Ma. There was a moderately long period of non-vertical motion in the location of Epiya – 1, which lasted for 1.17 Ma. This was accompanied by high subsidence rate (688.8 m/Ma), which lasted for a short period of 0.39 Ma. There was no significant vertical motion recorded after this last phase of subsidence. Three episodes of local tectonic events were recorded in the location of Ayetoro – 1; they include two periods of subsidence interrupted by a period of uplift. These two phases of subsidence occurred at a rate of 587.2 m/Ma and 221.6 m/Ma, while the uplift occurred at a rate of 119.1 m/Ma. The last phase of the subsidence extended to the beginning of Pleistocene. The Pliocene sedimentary succession was deposited in shelf marine environments ranging from inner to middle neritic. Sedimentation rate was high (Baba – 1.187 m/Ma; 193 m/Ma; Ayetoro -1.344 m/Ma; and Epiya – 1.260 m/Ma) and balanced up with the high subsidence rate recorded during this period. This possibly was responsible for the progressive shallowing of water depth that occurred during this period.

Data were only available in two wells (Baba – 1 and Ayetoro -1) to document the Quaternary tectonic events in the area. These events were characterised by extremely high periods of subsidence and minor periods of uplift. In Ayetoro – 1, these events have the following subsidence rates: 221.6 m/Ma, 1339.3 m/Ma, 1549.1 m/Ma and 156.2 m/Ma. Also recorded was an episode of non-vertical motion and another episode of uplift at a rate of 357.1 m/Ma. Five events were recorded in Baba – 1, characterised by variable subsidence rates and one episode of uplift. These rates occur in the following order: 1096 m/Ma, 121.8 m/Ma, 1948.8 m/Ma and 1218 m/Ma. The uplift episode has a rate of 121.8 m/Ma. Sedimentary succession during Quaternary was deposited in shelf marine environments ranging from inner to middle neritic, which is similar to previous environments. Sedimentation rate was extremely high being the highest recorded in all the wells. The rates in Baba – 1 and Ayetoro – 1 are 588 m/Ma and 797 m/Ma, respectively. The sedimentation rate was balanced with the high subsidence rate recorded in the Quaternary. This resulted in progressive shallowing of water depth

and progradation of facies. Essential trends of events Epoch by Epoch in the three wells are presented in Tables 4, 5 and 6.

Table 4. Relationship between basin tectonics and geological Epoch in Epiya – 1.

Age	Lithology	Ztect	LdSub	Ztotal	Basin Tectonics
Early Pliocene	Sandstone	4246	2	4248	
Early Pliocene	Shale	4183	3	4186	Subsidence
Early Pliocene	Sandstone	4175	27	4202	Quiescence
Early Pliocene	Shale	4135	68	4203	Quiescence
Early Pliocene	Sandstone	3943	3	3945	Subsidence
Early Pliocene	Shale	3939	5	3943	Quiescence
Early Pliocene	Sandstone	3926	2	3928	Subsidence
Early Pliocene	Shale	3923	13	3936	Subsidence
Early Pliocene	Sandstone	3888	5	3893	Subsidence
Early Pliocene	Shale	3880	70	3950	Uplift
Late Miocene	Shale	3785	74	3860	Subsidence
Middle Miocene	Shale	3462	62	3524	Subsidence
Middle Miocene	Siltstone	3326	4	3330	Subsidence
Middle Miocene	Shale	3252	34	3286	Subsidence
Early Miocene	Shale	3302	137	3439	Uplift
Early Miocene	Sandstone	2805	6	2811	Subsidence
Early Miocene	Shale	2790	12	2802	Subsidence
Early Miocene	Sandstone	2697	24	2721	Subsidence
Early Miocene	Shale	2711	31	2742	Subsidence
Early Miocene	Sandstone	2562	15	2577	Subsidence
Early Miocene	Shale	2534	130	2663	Uplift
Oligocene	Shale	2227	79	2305	Subsidence
Eocene	Shale	2031	11	2042	Subsidence
Eocene	Sandstone	2002	3	2005	Subsidence
Eocene	Shale	1926	27	1953	Subsidence
Eocene	Sandstone	1927	8	1936	Subsidence
Eocene	Siltstone	1757	6	1763	Subsidence
Eocene	Shale	1744	9	1753	Subsidence
Paleocene	Shale	1885	238	2123	Uplift
Paleocene	Siltstone	1261	14	1274	Subsidence
Paleocene	Shale	1112	26	1138	Subsidence
Paleocene	Siltstone	1020	20	1040	Subsidence
Paleocene	Shale	982	13	995	Subsidence
Paleocene	Sandstone	950	6	956	Subsidence
Early Maastrichtian	Shale	983	13	997	Uplift
Early Maastrichtian	Siltstone	901	26	927	Subsidence
Early Maastrichtian	Shale	779	89	869	Subsidence
Early Maastrichtian	Sandstone	633	5	637	Subsidence
Campanian	Shale	548	61	608	Subsidence
Santonian	Shale	584	12	596	Subsidence
Coniacian	Shale	687	18	706	Uplift
Turonian	Shale	649	51	701	Subsidence
Turonian	Siltstone	592	50	642	Subsidence
Cenomanian	Shale	425	66	491	Subsidence
Cenomanian	Sandstone	38	53	90	Subsidence
Cenomanian	Shale	39	74	113	Uplift
Cenomanian	Sandstone	-121	49	-72	Subsidence
Cenomanian	Shale	-241	21	-221	Subsidence

Table 5. Relationship between basin tectonics and geological Epoch in Ayetoro – 1.

Age	Lithology	Ztectonics	LoadSub	Ztotal	Basin Tectonics
Pleistocene	Sandstone	3575.5	11.1	3586.7	
Pleistocene	Shale	3560.1	16.2	3576.3	Subsidence
Pleistocene	Sandstone	3517.9	14.4	3532.3	Uplift
Pleistocene	Shale	3497.8	45.0	3542.8	Subsidence
Pleistocene	Sandstone	3380.2	8.6	3388.7	Subsidence
Pleistocene	Shale	3368.2	21.8	3390.0	Uplift
Pleistocene	Sandstone	3311.3	8.1	3319.4	Subsidence
Pleistocene	Shale	3300.1	57.1	3357.2	Quiescence
Pleistocene	Siltstone	3150.8	49.6	3200.3	Subsidence
Pleistocene	Sandstone	3044.7	24.6	3069.3	Subsidence
Pleistocene	Shale	3010.3	55.5	3065.8	Subsidence
Pleistocene	Sandstone	2863.0	18.6	2881.5	Subsidence
Pleistocene	Siltstone	2834.6	40.1	2874.7	Subsidence
Pleistocene	Shale	2746.3	20.4	2766.6	Subsidence
Pleistocene	Siltstone	2691.5	19.0	2710.5	Subsidence
Pliocene	Siltstone	2548.9	23.2	2572.1	Subsidence
Pliocene	Shale	2497.3	223.3	2720.6	Uplift
Pliocene	Shale	2017.7	25.1	2042.8	Subsidence
Upper Miocene	Shale	2003.8	42.5	2046.3	Subsidence
Upper Miocene	Shale	1896.0	4.2	1900.1	Subsidence
Upper Miocene	Shale	1860.5	21.0	1881.5	Subsidence
Upper Miocene	Siltstone	1808.2	9.0	1817.1	Uplift
Upper Miocene	Siltstone	1839.8	13.4	1853.3	Uplift
Middle Miocene	Siltstone	1901.2	55.1	1956.2	Uplift
Middle Miocene	Siltstone	1588.0	8.4	1596.4	Subsidence
Middle Miocene	Shale	1570.6	63.9	1634.4	Uplift
Middle Miocene	Shale	1409.4	26.0	1435.4	Subsidence
Middle Miocene	Shale	1545.7	22.0	1567.6	Uplift
Middle Miocene	Shale	1292.3	109.6	1401.9	Subsidence
Middle Miocene	Shale	1229.3	20.0	1249.4	Quiescence
Lower Miocene	Sandstone	1225.9	1.3	1227.1	Subsidence
Lower Miocene	Sandstone	1024.4	5.0	1029.4	Subsidence
Lower Miocene	Shale	1015.5	58.5	1074.0	Uplift
Lower Miocene	Siltstone	884.6	15.8	900.5	Subsidence
Lower Miocene	Siltstone	1056.6	8.6	1065.2	Uplift
Eocene	Siltstone	1117.4	31.9	1149.3	Uplift
Eocene	Sandstone	1061.0	5.7	1066.7	Subsidence
Eocene	Sandstone	854.4	10.4	864.8	Subsidence
Upper Paleocene	Shale	696.0	33.1	729.1	Subsidence
Upper Paleocene	Sandstone	623.5	24.7	648.2	Uplift
Upper Paleocene	Siltstone	670.0	29.3	699.3	Subsidence
Lower Paleocene	Siltstone	547.7	17.3	565.0	Uplift
Lower Paleocene	Siltstone	590.3	4.5	594.7	Subsidence
Lower Paleocene	Shale	581.8	79.2	661.0	Uplift
Maastrichian	Shale	402.8	37.1	439.9	Subsidence
Maastrichian	Shale	403.6	91.5	495.0	Uplift
Maastrichian	Sandstone	159.8	30.2	190.0	Subsidence
Maastrichian	Sandstone	213.3	17.9	231.3	Uplift
Upper Campanian	Sandstone	75.5	104.8	180.3	Subsidence

Table 6. Relationship between basin tectonics and geological Epoch in Baba – 1.

Age	Lithology	Ztect	LdSub	Ztotal	Basin Tectonics
Quaternary	Sandstone	4959	30	4989	
Quaternary	Shale	4987	12	4999	Uplift
Quaternary	Sandstone	4818	12	4830	Subsidence
Quaternary	Shale	4800	5	4805	Subsidence
Quaternary	Sandstone	4784	12	4796	Subsidence
Quaternary	Shale	4765	14	4779	Subsidence
Quaternary	Sandstone	4726	25	4751	Subsidence
Quaternary	Siltstone	4688	16	4703	Subsidence
Quaternary	Sandstone	4650	15	4665	Subsidence
Quaternary	Shale	4627	83	4711	Uplift
Quaternary	Sandstone	4381	24	4405	Subsidence
Quaternary	Shale	4342	19	4361	Subsidence
Quaternary	Sandstone	4193	11	4204	Subsidence
Upper Pliocene	Shale	4175	21	4196	Subsidence
Upper Pliocene	Sandstone	4203	3	4207	Uplift
Upper Pliocene	Shale	4198	18	4215	Uplift
Upper Pliocene	Sandstone	4145	6	4151	Subsidence
Upper Pliocene	Shale	4135	42	4178	Uplift
Upper Pliocene	Sandstone	4057	6	4063	Subsidence
Upper Pliocene	Shale	4047	16	4063	Quiescence
Upper Pliocene	Sandstone	3998	23	4022	Uplift
Lower Pliocene	Shale	3961	61	4021	Uplift
Lower Pliocene	Siltstone	3615	12	3627	Subsidence
Lower Pliocene	Shale	3584	52	3636	Uplift
Lower Pliocene	Siltstone	3499	6	3505	Subsidence
Lower Pliocene	Shale	3684	164	3848	Uplift
Upper Miocene	Shale	3219	37	3256	Subsidence
Upper Miocene	Sandstone	3107	7	3113	Subsidence
Upper Miocene	Shale	2938	93	3031	Subsidence
Middle Miocene	Shale	2659	294	2953	Subsidence
Lower Miocene	Shale	1603	68	1671	Subsidence
Lower Miocene	Siltstone	1603	15	1618	Subsidence
Lower Miocene	Shale	1582	23	1605	Subsidence
Upper Paleocene	Shale	1362	50	1412	Subsidence
Upper Paleocene	Siltstone	1022	7	1030	Subsidence
Upper Paleocene	Shale	1171	42	1213	Uplift
Upper Paleocene	Siltstone	934	8	941	Subsidence
Upper Paleocene	Shale	889	96	984	Uplift
Lower Paleocene	Shale	633	26	659	Subsidence
Lower Paleocene	Siltstone	568	16	584	Subsidence
Lower Paleocene	Shale	535	27	562	Subsidence
Lower Paleocene	Siltstone	469	7	476	Subsidence
Lower Paleocene	Shale	455	101	556	Uplift
Maastrichtian	Siltstone	278	55	333	Subsidence
Maastrichtian	Sandstone	132	8	140	Subsidence
Maastrichtian	Shale	-23	24	1	Subsidence
Maastrichtian	Sandstone	-10	12	2	Uplift
Upper Campanian	Shale	-26	63	37	Subsidence
Upper Campanian	Sandstone	-155	75	-80	Subsidence

CONCLUSION

A quantitative study of subsidence analysis in the Nigeria sector of the Benin (Dahomey) Basin has been presented using three offshore wells. The subsidence analysis was carried using one-dimensional backstripping technique. The results obtained showed that a cogent analysis of tectonic subsidence is feasible in the study area, even though the sedimentary successions contain diverse, fully lithified siliciclastic rocks. Biostratigraphic data in one of the wells (Epiya – 1) indicated that the oldest sediment penetrated is Cenomanian, while in Baba – 1 and Ayetoro – 1 the oldest sediments were Campanian in age. The subsidence patterns indicated that Early late Cretaceous phase (Cenomanian to Campanian) was characterised by accelerated tectonic subsidence and gradual uplift patterns. The Late Cretaceous phase (Campanian to Maastrichtian) exhibited relatively high uniform rates of subsidence and minor uplift. Maastrichtian to Paleocene subsidence is recorded by all the curves obtained in the three wells. The most apparent features, which are practically ubiquitous in all the curves are the Maastrichtian to Paleocene subsidence and Eocene uplift. Uplift is contemporaneous with observed Eocene/Oligocene unconformity recorded in two wells (Baba – 1 and Ayetoro – 1), therefore, a genetic relation probably occurred between the two phenomena. The Paleogene to Neogene phases showed variable rates of tectonic subsidence and uplift while the Quaternary began with accelerated tectonic subsidence followed by reduced rates of tectonic subsidence. Some periods of basin quiescence were observed during Miocene and Pliocene times. This type of study is important at this stage of the Benin (Dahomey) Basin, especially with the discovery of hydrocarbons in the offshore section and the linkage of the basin with transform faults.

ACKNOWLEDGEMENT

Special thanks go to Chevron Nigeria Limited for releasing the data used for this study.

REFERENCES

Ajakaiye, D.E. and Bally, A.W., 2002. Course manual and atlas of structural styles on reflection profiles from the Niger Delta. *American Association of Petroleum Geologists,* Continuing Education Course Note Series, no. 41, 107pp.

Adegoke, O. S. 1969. Eocene Stratigraphy of southern Nigeria. *Collogue sur Eocene v. III Bur. Rech. Geol. Min. Mem.*, no. 69, p. 23 – 48.

Billman, H. G. 1992. Offshore stratigraphy and paleontology of Dahomey (Benin) Embayment. *Nigerian Association of Petroleum Explorationists Bulletin*, v. 70, no. 02, p. 121- 130.

Bond, G.C. and Kominz, M.A. 1984. Construction of tectonic subsidence curves for the early Paleozoic miogeocline, southern Canadian Rocky Mountains: implications for subsidence mechanisms, age of break-up and crustal thinning. *Geological Society of America Bulletin*, v. 95, 155– 173.

Brownfield M.E and Charpentier R.R. 2006. Geology and Total Petroleum Systems of the Gulf of Guinea Province of West Africa *U.S. Geological Survey Bulletin* 2207-C.

Burke, K.; MaCgregor, D. S. and Cameron, N. R. 2003. *In* Arthur, T.J., MaCgregor, D. S. and Cameron, N. R. (Edited), Petroleum Geology of Africa: New Themes and Developing Technologies. *Geological Society, London,* Special Publications, v. 207, p. 21-60.

Carminati, E.; Corda, L.; Mariotti, G., and Brandano, M. 2007. Tectonic control on the architecture of a Miocene carbonate ramp in the Central Apennines (Italy): Insights from facies and backstripping analyses. *Sedimentary Geology*, v. 198, 233–253.

Ceramicola, S.; Stoker, M.; Praeg, D.; Shannon, P.M.; De Santis, L.; Hoult, R.; Hjelstuen, B.O.; Laberg, S. and Mathiesen, A. 2005. Anomalous Cenozoic subsidence along the 'passive' continental margin from Ireland to mid-Norway. *Marine and Petroleum Geology* v. 22, 1045–1067.

Coker, S.J. L. 2002. Field excursion guide to tar sand outcrops in Benin Basin. *Nigerian Association of Petroleum Explorationists*, Mini-Conference, 32 pp.

Coker, S. J. L. and Ejedawe, J. E. 1987. Petroleum prospect of the Benin basin Nigeria.

Journal of Mining and Geology, v. 23(01), p. 7 – 43.

Coker, S. J. L. and Ejedawe, J. E. 1987. Petroleum prospect of the Benin basin Nigeria. *Journal of Mining and Geology,* v. 23(01), p. 7 – 43.

Coudert, L.; Frappa, M.; Viguier, C. and Arias, R. 1995. Tectonic subsidence and crustal flexure in the Neogene Chaco basin of Bolivia. *Tectonophysics*, 243, 277–292.

Haack, R.C.; Sundararaman, P.; Diedjomahor, J.O.; Xiao, H.; Gant, N.J.; May, E.D. and Kelsch, K. 2000. Niger Delta petroleum systems, Nigeria, *in* Mello, M.R., and Katz, B.J., (Edited), Petroleum systems of South Atlantic margins. *American Association of Petroleum Geologists*, Memoir 73, p. 213–231.

Haq, B. U.; Hardenbol, J. and Vail, P. 1988, Mesozoic and Cenozoic chronostratigraphy and cycles of relative sea level change, in C. Wilgus, B. Hastings, C. Kendall, H. Posamentier, C. Ross, and J. Van Wagoner, eds., Sea level changes: An integrated approach: *Society Economic Paleontologists and Mineralogists,* Special Publication, 42, p. 3– 17.

http://atlas.geo.cornel.edu. Tectonic subsidence notes.

Jones, H.A and Hockey, R. D. 1964. The Geology of part of Southwestern Nigeria. *Geological Survey of Nigeria Bulletin,* v. 31, 101p.

Kusznir, N.J.; Roberts, A.M. and Morley, C., 1995. Forward and reverse modelling of rift basin formation. In: Lambiase, J. (Ed.), Hydrocarbon Habitat in Rift Basins. *Geological Society, London,* Special Publications, v. 80, p. 33–56.

Ogbe, F. G. A. 1972. Stratigraphy of the strata exposed in the Ewekoro quarry, western Nigeria. In Dessauvagie, T.F.J. and Whiteman, A.J., eds., *African Geology,* University Press, Nigeria, 3050322.

Omatsola, M. E. and Adegoke O. S. 1981. Tectonic evolution and Cretaceous stratigraphy of the Dahomey basin, Nigeria. *Journal of Mining and Geology,* v. 18(01), p. 130 -137.

Onuoha, K.O. 1999. Structural features of Nigeria's coastal margin: an assessment based on age data from wells. *Journal of African Earth Sciences*, v. 29/ 03, p. 485-499.

Onuoha, K.O. and Ofoegbu C.O. 1987. Subsidence and evolution of Nigeria's continental margin: implications of data from Afowo – 1 well. *Marine and Petroleum Geology,* v. 5, p. 175 – 181.

Reyment, R. A. 1965. Aspects of the geology of Nigeria – the stratigraphy of the Cretaceous and Cenozoic deposits. *Ibadan University Press*, 133pp.

Sclater, J.G. and Christie, P.A.F., 1980. Continental stretching: an explanation of the post-mid-Cretaceous subsidence of the central North Sea basin. *Journal of Geophysical Research*, v. 85 (B7), p. 3711 –3739.

Steckler, M.S. and Watts, A.B., 1978. Subsidence of the Atlantic-type continental margin off New York. *Earth Planetry Science Letters*, v. 41, p. 1 –13.

Van Hinte, J.E. 1978. Geohistory analysis Application of micropaleontology in exploration geology. *American Association of Petroleum Geologists Bulletin,* v. 62(2), p. 201-222.

Wagreich, M. and Schmid, H.P., 2002. Backstripping dip–slip fault histories: apparent slip rates for the Miocene of the Vienna Basin. *Terra Nova*, 14, 163–168.

Watcharanantakul, R. and Morley, C.K., 2000. Syn-rift and post-rift modelling of the Pattani Basin, Thailand: evidence for ramp-flat detachment. *Marine and Petroleum Geology,* v. 17, p. 937– 958.

Weber, K.J. and Daukoru, E. 1975. Petroleum geology of the Niger Delta. *Ninth World Petroleum Congress,* 2, p. 209-221.

Whiteman, A. 1982. Nigeria: Its petroleum geology, resources and potential. *Graham and Trotman,* 394p.

Wilson R. C. C. and Willians, C. A. 1979. Oceanic transform structures and the developments of Atlantic continental margin sedimentary basin a review. *Journal of Geological Society of London,* v. 136, p. 311 – 320.